Task Oriented Nonlinear Control Laws for Telerobotic Assembly Operations

R.A. Walker,† L.S. Ward,* and C.F. Elia*
Integrated Systems, Inc.
Palo Alto, CA 94301

Abstract

The goal of this research is to achieve very intelligent telerobotic controllers which are capable of receiving high-level commands from the human operator and implementing them in an adaptive manner in the object/task/manipulator workspace. This paper presents initiatives by the authors at Integrated Systems, Inc. to identify and develop the key technologies necessary to create such a flexible, highly programmable, telerobotic controller. The focus of the discussion is on the modeling of insertion tasks in three dimensions and nonlinear implicit force feedback control laws which incorporate tool/workspace constraints. Preliminary experiments with dual arm beam assembly in 2D are presented.

I. Introduction

In the future, telerobotic manipulators will be used to enable increased space assembly, servicing, and repair. Specific goals, as determined by NASA, are:

1) "to decrease mission operations manpower by 75 percent,
2) to replace 50 percent of extravehicular activity (EVA) with telerobotics, and
3) to enable remote (e.g. geosynchronous earth orbit and polar orbit) assembly, servicing, and repair through telerobotics" [1].

In order to satisfy the above requirements for telerobotics, significant improvements in manipulator control will be necessary. Telerobotic assembly requires powerful locally autonomous control laws for 1)task completion in the presence of disturbances and sensor errors 2) control of position and force for trajectory guidance 3) task completion without continuous operator supervision. The last is especially important for long distance tasks (such as Mars exploration) where the time delays involved in receiving sensory information or relaying earth-based control signals make traditional teleoperation unsuitable. Furthermore, an interface for expert system planners and/or human interaction will be necessary so that the system is flexible to various levels of human supervision.

Previous work in the general area of robotics has focused on a decompositon of robot control into trajectory planning and servocontrol to the preplanned wire in statespace. A logical extension of this work approaches the problem with real-time expert systems to formulate the planned trajectory "in-the-loop". Expert systems "in-the-loop" will be much more powerful with more sophisticated control algorithms as a foundation. Namely, analytic, optimization based, "trajectory feedback", nonlinear control laws whose performance index and time phasing are controlled by a combination of expert systems and the human operator.

The effort described below involves fundamental nonlinear control laws valuable in dual arm coordination. These approaches to dextrous, coordinated motion were evaluated in a new highly flexible simulation environment [2]. The authors have modeled two 3DOF planar robots, performing a beam assembly task. Two dimensonal plots and figures illustrate by comparative results the sensitivity of performance to the control law structure. Reasonable long term research conclusions will be

a) which control approaches are most reasonable

b) what level of actuator/sensor performance is required to do meaningful experiments well with these control laws, and

† Manager, Aircraft and Robotics Control Systems Division
* Members of Technical Staff

c) what are the controller architecture issues to implement such control laws.

We first describe the modeling, then various control structures followed by a discussion of the experimental results.

II. Dual Arm Modeling

Modeling and Simulation Tools

The following research was carried out using MATRIX$_X$/AR (Automation and Robotics Modeling and Simulation Package)[2]. This tool provides a flexible modeling and simulation environment for manipulators, actuators, and control laws. Figure 1 is a flowchart for the use of MATRIX$_X$/AR. Model creation is initiated by using the menu-driven RUI (Robotic User Interface) to specify the geometric, inertial, and functional specifications of the manipulator. The RUI creates a robotic database from the given and computed data. This data is accessed by command files which build a kinematic and dynamic model of the manipulator using the recursive Newton-Euler approach. This model is created in SYSTEM_BUILD[3], a simulation/integration package where linear, nonlinear, and multirate systems and controllers can be modeled quickly and easily in a block diagram format. Figure 2 shows the inverse dynamic model of the PUMA 560 with blocks for the base, arm, wrist, and end effector. The blocks are nested, so that the block for the arm contains blocks for link 1, link 2, and link 3, each of which contains a dynamic, kinematic, and actuator block. By using input flags, the PUMA block can be used to obtain kinematic, dynamic, and inverse dynamic information. Suitable control laws can be generated by using classical and modern control design techniques available in MATRIX$_X$/AR. The plant and control models are combined in an overall system which is then simulated. Post-processing animation capabilities are used to visualize the success or failure of a particular controller.

Manipulator Robot Models

Each of the two robotic manipulators modeled in this study is a three DOF articulated arm. The arms are made up of three rigid links connected through one prismatic and two revolute joints. Since the first and second joint axes are perpendicular, and the second and third are parallel, each arm moves in a plane with one translational and two rotational degrees-of-freedom. A schematic of an arm is shown in Figure 3.

The 3-DOF planar manipulators are identical, with the physical characteristics shown in Table 1.

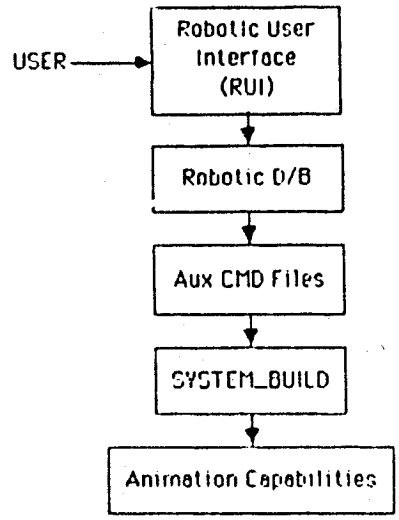

Figure 1. MATRIX$_X$/AR Design Flowchart.

Space Assembly Beam Model

The mating of two long slender beams was chosen as a suitable test for the proposed control algorithms. The beams were sized relative to the arms to simulate a truss assembly scenario. The beams, as well as the manipulators, have a

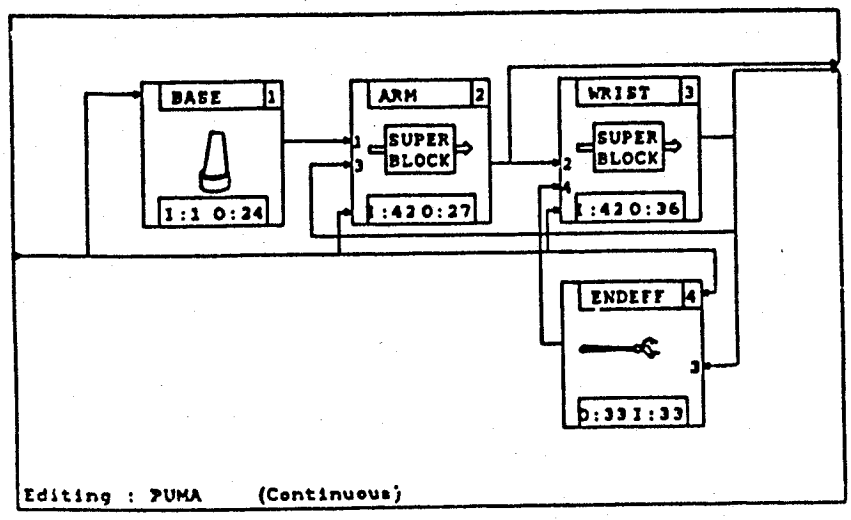

Figure 2. Model of PUMA 560.

cylindrical (hollow) shape with the dimensions shown in Table 1.

The dual arm configuration, complete with beams, is shown in its initial position in Figure 4. The arm and beam on the left with the socket will be referred to as Manipulator 1, and those on the right with the peg as Manipulator 2. The

Table 1
3-DOF Planar Manipulator Physical Characteristics.

	Link 1	Link 2	Link 3	Beam
Geometric Properties				
Joint Type	Swivel	Sliding	Hinge	n/a
Length (m)	.2	.4	.4	1
Cylinder:				
Inner Radius (m)	.046	.0335	.0335	.023
Outer Radius (m)	.050	.0375	.0375	.025
Inertial Properties				
Mass (Kg)	.724	1.07	1.07	.905
Inertias (Kg-m^2):				
I_{xx}	.0017	.0014	.0014	.0005
I_{yy}	.0032	.0149	.0149	.0757
I_{zz}	.0032	.0149	.0149	.0757

desired goal involves inserting a peg on the left end of the second beam into the hole in the middle of the first beam.

Dual Arm Constraint Model

Simulating closed dynamic chains, such as the dual arm manipulators during an assembly task, is a difficult problem. The collisions which occur during insertion result in abrupt changes in the motion (velocity) states. These discontinuities cause problems for the integration package. The problem is dealt with in this research by using a compliant model, since there is, naturally, compliance in any mechanical mechanism. For this work, the first arm, second arm, and second beam

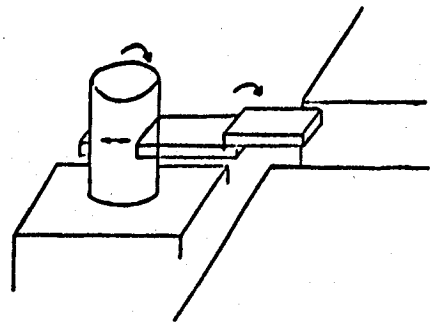

Figure 3. Schematic of Three DOF Arm.

are treated as being rigid. The hole and the second beam are compliant, generating an opposing force linearly proportional to the amount of deflection caused by the inserting peg upon collision. Since computer CPU time is dependent upon the "stiffness" of the equations, preliminary tests are run using relatively low spring constants. The results described below are in this category, with spring gains of 1000 N/m.

III. Dual Arm Control

This section gives an overview of the various aspects of the control approaches investigated on a dual arm experiment.

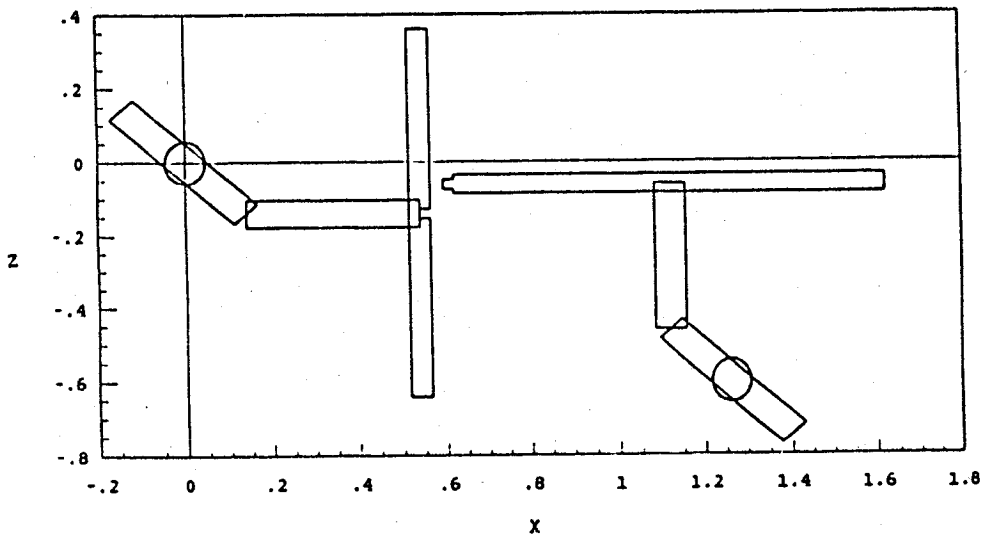

Figure 4. Dual Arm Configuration.

3.1 Control Design

The performance of a robotic manipulator in a compliant task, such as peg insertion, greatly depends on the choice of control used. A one-step control law based on previous research [4] was used for the beam assembly problem described above.

The advantage of this scheme over typical hybrid force/position control is that the control law works for both constrained and unconstrained motion; thus, the peg does not need to be in close proximity to the hole initially. A brief description of the control law is presented below.

Nonlinear Control

The equation of the motion of the end effector in cartesian space is given by

$$\Lambda(x)\ddot{x} + \mu(x,\dot{x}) + p(x) = F \tag{1}$$

where x is a vector of position and orientation, $\mu(x,\dot{x})$ contains the Coriolis and centripetal terms, and $p(x)$ contains the gravity terms. A nonlinear control law can be used to globally linearize equation (1) [5]. The result is a linear system of the form

$$\ddot{x} = F_c. \tag{2}$$

Multiplying (2) on both sides by $\Lambda(x)$ and adding $\mu(x,\dot{x}) + p(x)$ gives

$$\Lambda(x)\ddot{x} + \mu(x,\dot{x}) + p(x) = \Lambda(x)F_c + \mu(x,\dot{x}) + p(x)$$

Letting $F = \Lambda(x)F_c + \mu(x,\dot{x}) + p(\dot{x}) = \Lambda(x)F_c + F_d$, where $F_d = \mu(x,\dot{x}) + p(x)$, the feedback is composed of two components: a component containing the feedback law designed for the linear system (2), and a nonlinear decoupling component based on the nonlinear terms of (1). It is important to note that exact nonlinear control requires a precise model of the manipulator.

Constrained Motion Control

Control in the presence of constraints was based on research done by Ish- Shalom [6]. The method involves specifying a task constraint and then using that constraint as the optimization criterion for a linear quadratic optimal control design. For example, the constraint on the end effector force and velocity

$$f \cdot v = 0$$

describes sliding along a surface. A linear quadratic controller can be designed to satisfy this constraint. It is based on minimizing the performance index

$$J = ||f \cdot v||^2 = v^T H(f) v$$

and is derived for system (2) with the following result [4]:

$$F_c = -Kx$$

$$\begin{aligned} K &= [K_p \quad K_v] \\ &= [0 \quad \tfrac{1}{\sqrt{\alpha}} H(f)] \end{aligned}$$

where K_p is positional feedback, K_v is velocity feedback, α is a constant, and

$$H(f) = \begin{bmatrix} f_x^2 & f_x f_y & f_x f_z \\ f_x f_y & f_y^2 & f_y f_z \\ f_x f_z & f_y f_z & f_z^2 \end{bmatrix} \geq 0 \qquad \forall f \in R^3$$

Note that the force is controlled implicitly through the velocity feedback.

Unconstrained Motion Control

Control in the absence of constraints can be determined by using linear quadratic optimal control. The solution for system (2) will provide position and orientation control for the manipulator.

3.2 Dual Arm Beam Assembly Control Strategies

The three control laws described above were combined and used with the dual arm configuration described in chapter 2. Three preliminary control strategies, shown in Table 2, were chosen to determine preliminary conclusions on the importance of implicit force control and relative vs. global cooperative control schemes.

Table 2
Dual Arm Control Strategies Simulated

Ex.	Control Strategies	
#	arm 1 *(Socket Receptor)*	arm 2 *(Insertion Peg)*
1	NL global servo	NL-force global servo
2	NL-force global servo	NL-force global servo
3	NL-force global/ local servo	NL-force global servo

A global servo means the control is servoing to a point in inertial space. A local servo means that one arm servos relative to the other arm. The nonlinear aspect is what is often called the coupled torque method, and the force control is all implicit based on the constraint modeling described above. The next section describes the motivation for these strategies and experimental simulation results.

IV. Dual Arm Simulation Results

The first experiment tests the performance of control laws without coordination. The second experiment adds implicit force control to give a local coordination effect, and the third shows how significant passing information on the other arm's activity is to accomplish a coordinated assembly task.

Experiment 1 Objectives and Results

In experiment 1 both arms were servoed to a globally defined position and orientation. The defined position for both arms corresponds to the base point of the hole in the beam attatched to arm 1. Arm 2 was controlled by the combined controller as described above. Arm 1 however, did not have implicit force control. The simulation results are shown for successive time frames in Figure 5. Note that the initial contact of arm 2 onto arm 1 caused significant deflection, so that mating was only possible after a second attempt.

Experiment 2 Objectives and Results

Experiment 2 was the same as the experiment 1 with the exception that arm 1 was given implicit force control. As can be seen in Figure 6, the mating was accomplished in the first try. This is due to the cooperative motion of the manipulators after contact, even though they had no information about each others positions and were servoed to a globally defined point in space. The presence of the implicit force in arm 1 caused that arm to move in the positive z direction after being hit by arm 2 (perpendicular to the direction of the external force) rather than in the -x direction as before. Thus, local relative movement (away from the defined servo point) occured with arm 1 which allowed the two beams to mate faster and then travel back together to the global servo point.

Experiment 3 Objectives and Results

Experiment 3 was the same as experiment 2 with the exception that arm 1 was given information about the z component of the peg's location (attatched to arm 2). Arm 1 was thus servoed globally in the x direction and relatively (to arm 2) in the z direction. As can be seen in Figure 7, faster mating was obtained due to global movement of arm 1.

Simulation Experiment Summary and Conclusions

It should be noted that the above experiments represent preliminary results run under idealized conditions. The nonlinear control was exact and the hole was modeled compliantly as a spring system, allowing the manipulator to penetrate the first beams surface and then apply a point force proportional to the maximum penetration. These simulations were designed, however, to illustrate the potential benefit of using nonlinear implicit force feedback. Two key observations can be made.

First, the presence of implicit force feedback in both arms demonstrated how the two arms were capable of moving cooperatively without any knowledge of each other. The implicit force feedback allowed local movement about the globally defined servo point, which resulted in cooperative relative movement for the arms. This is extremely valuable since this can compensate for sensor inaccuracies in specifying and measuring the global servo point.

Second, as should be obvious, giving one or both arms information about each other, such as positional information, allows a greater degree of cooperation in the assembly task. Thus, future research will concentrate on using cooperative schemes, such as dual arm one-sided optimal guidance, to increase the amount of cooperation between the two arms.

V. Summary

This paper has outlined telerobotic research in progress at Integrated Systems. The emphasis on the work has been to develop goal directed guidance laws which provide a more powerful framework for telerobotic planners and teleoperator controllers to interface. Preliminary work has been done to test the concepts by simulation, using flexible automation modeling and control tools developed at Integrated Systems.

The dual arm control laws tested show that the control strategy is very important for assembly operations and could be of great benefit to NASA's space bound manipulators. Since there is a major need for telerobots to possess significant decision-making capabilities before they can be used extensively in remote and hazardous situations, it will be valuable in the industrial and nuclear environments as well.

References

[1] M.D. Montemerlo, "NASA's Automation and Robotics Technology Development Program," *Proc. of 1986 IEEE International Conference on Robotics and Automation*, San Francisco, CA, April 7-10, 1986.

[2] Reza Langari, Robert A. Walker, Norm Coleman, and Pak Yip, "A Robotics Modeling and Control Law Development Environment," *Proceedings of the AIAA Guidance Control Conference*, Williamsburg, VA, August 18-20 1986.

[3] N.K. Gupta, D. Varvell, and R.A. Walker, "SYSTEM_BUILD: A New Interactive Model Building and Simulation CAE Tool," *Proc. of the Society for Computer Simulation*, July 22-24, 1985.

[4] Reza Langari and Robert A. Walker, "Nonlinear Feedback Strategies for Control of Robotic Manipulators," ISI Technical Memorandum 6507-002, March 1986.

[5] E. Freund, "Fast Nonlinear Control with Arbitrary Pole Placement for Industrial Robots and Manipulators," *Robotics Research 1*, MIT Press 1982.

[6] J. Ish-Shalom, "The C.S. Language Concept: A New Approach to Robot Motion Design," International Journal of Robotics Research, Spring 1985, pp. 42-58.

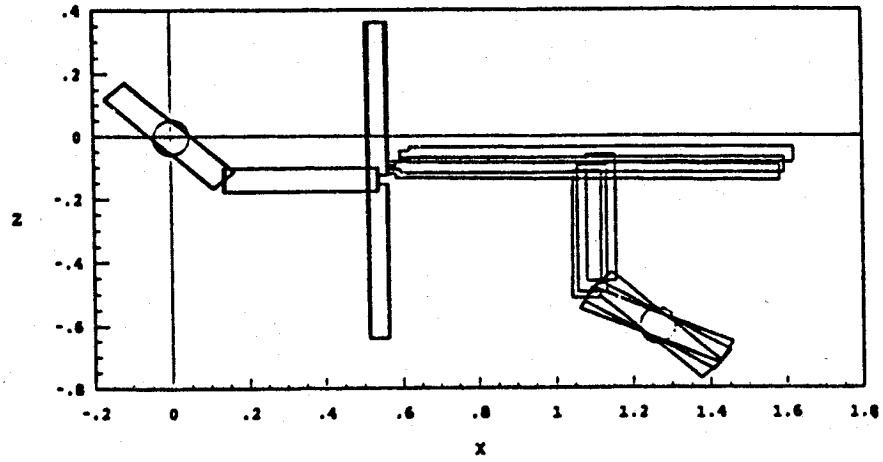

Figure 5a).

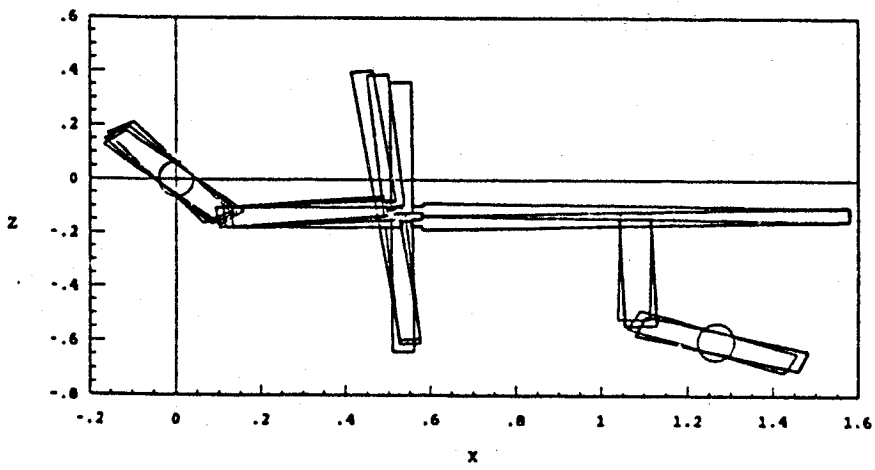

Figure 5b).

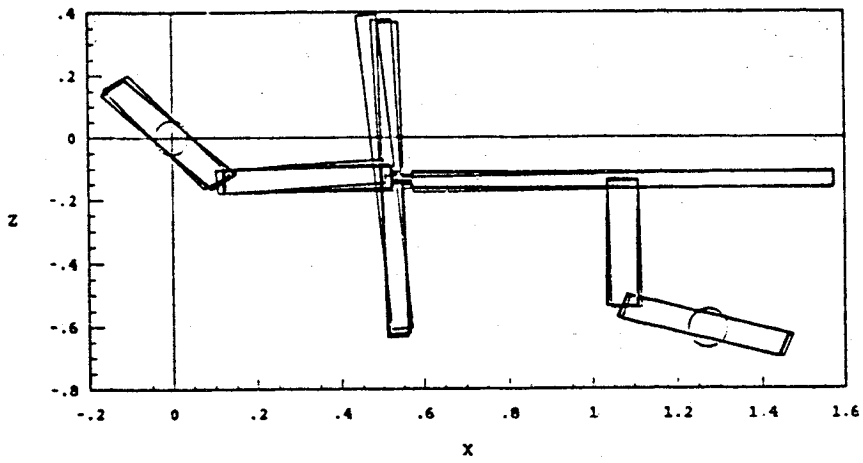

Figure 5c).

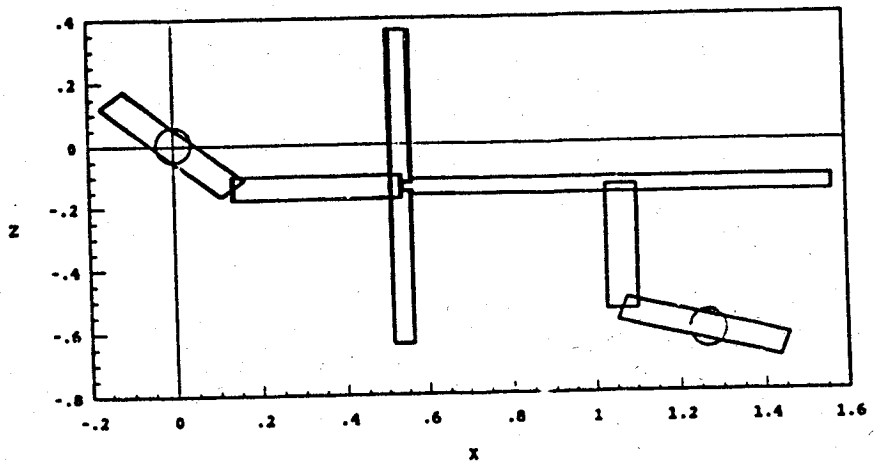

Figure 5d).

Figure 5). Experiment 1 Results - Global Servoing With One-Sided Implicit Force Coordination (see Table 2) a) 0-1.75 secs, b) 2.25-3.25 secs, c) 3.75-6.0 secs, d) 6.75-9 secs.

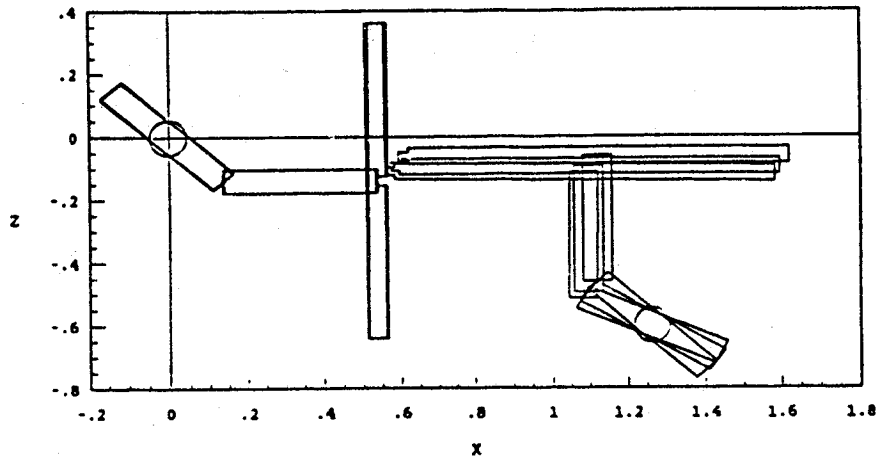

Figure 6a).

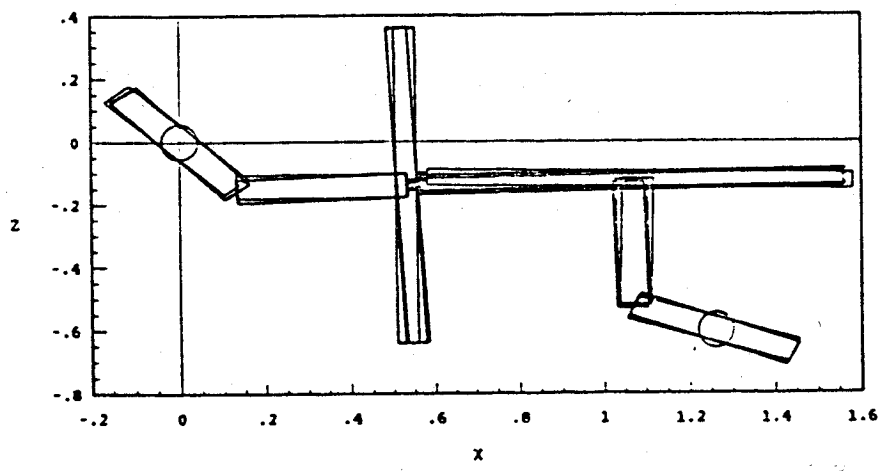

Figure 6b).

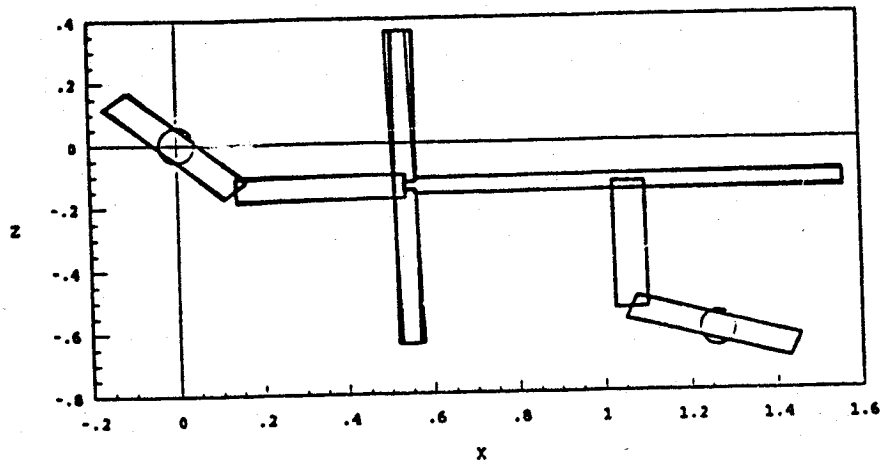

Figure 6c).

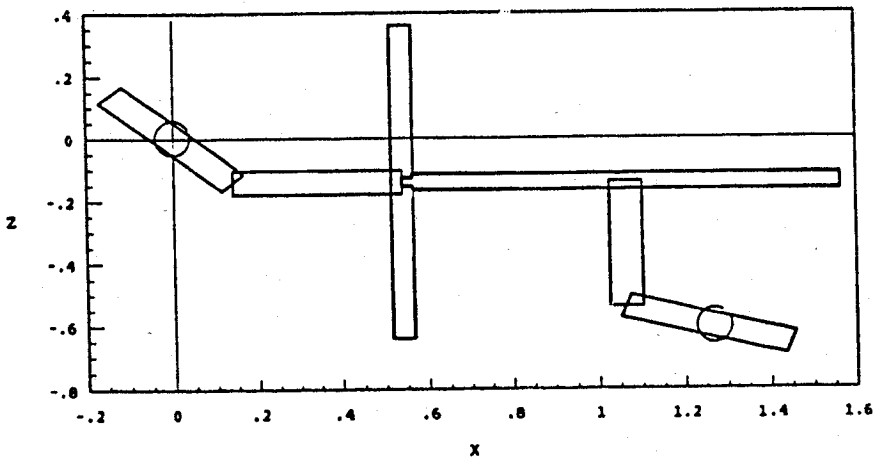

Figure 6d).

Figure 6). Experiment 2 Results – Global Servoing With Two-Sided Implicit Force Coordination (see Table 2) a) 0-1.75 secs, b) 2.25-3.25 secs, c) 3.75-6.0 secs, d) 6.75-9 secs.

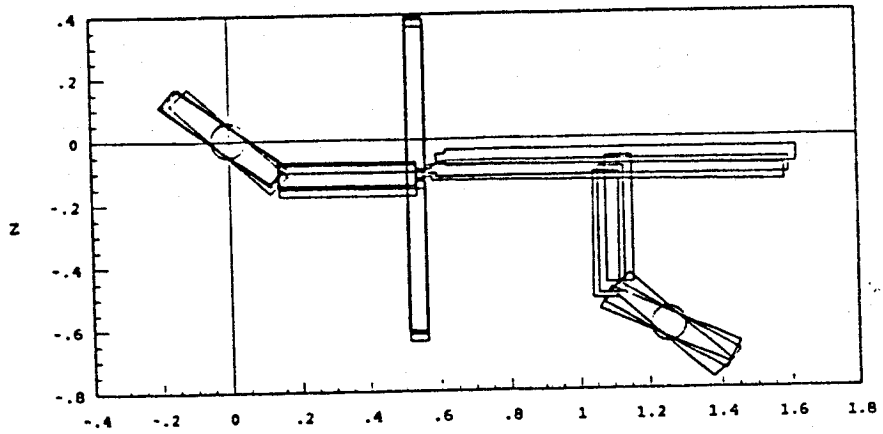

Figure 7a).

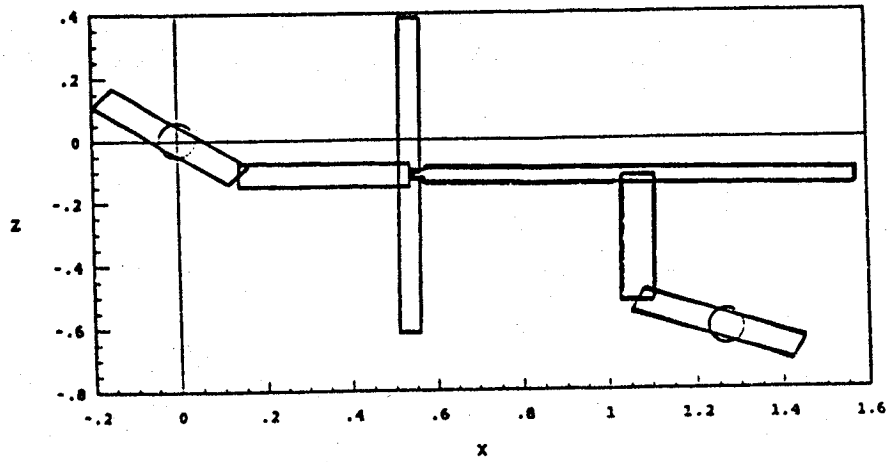

Figure 7b).

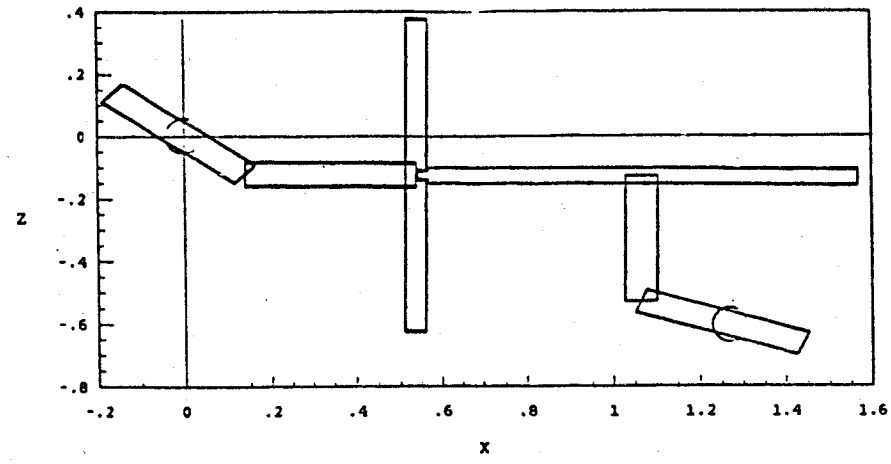

Figure 7c).

Figure 7). Experiment 3 Results - Global and Local Servoing With Two-Sided Implicit Force Coordination (see Table 2)

a) 0-1.75 secs, b) 2.25-3.25 secs, c) 3.75-6.0 secs.